Earthquake Geotechnical Engineering for Protection and Development of Environment and Constructions – Silvestri & Moraci (Eds)
© 2019 Associazione Geotecnica Italiana, Rome, Italy, ISBN 978-0-367-14328-2

Stratigraphic amplification factors based on parametric 1D site response analyses and KiK-net downhole recordings: Evaluation and comparison with code provisions

A. Pagliaroli, V. Papa & I. Pisotta
Dipartimento di Ingegneria e Geologia, Università degli Studi "G. d'Annunzio" di Chieti Pescara, Italy

ABSTRACT: The aim of paper is to assess the performance of stratigraphic amplification factors S_S as specified by the Italian National Technical code NTC18. The variation of S_S with input PGA, taking therefore into account soil nonlinearity, was assessed by means of about 2800 parametric numerical 1D site response analyses carried out on virtual soil profiles as well as from the processing of more than 5500 recordings from Japanese KiK-net stations. The stratigraphic factors were computed in terms of PGA as well as ratio of integral spectral amplitude in the range of period 0.05-2.5s. The results of parametric numerical analyses indicate that NTC18 is too conservative for subsoil class D in the whole range of input PGA; the opposite is observed for class E where NTC18 shows a significant underestimation of seismic response. Moreover, the NTC18 foresees an excessive enlargement of the spectra towards the high periods for all the classes due to an overestimation of the shape parameter C_C. The empirical amplification factors are quite higher than numerical ones especially at low values of input PGA: this behavior has been ascribed to the high stiffness of bedrock encountered in the KiK-net profiles, well above the V_S=800 m/s assumed for numerical schemes and in the NTC18 code.

1 INTRODUCTION

Advanced technical codes have largely accepted the importance of local site conditions in modifying the seismic actions (NEHRP, 1991; CEN, 2004; Ministero delle Infrastrutture e dei Trasporti, 2018). The execution of site response analyses is highly recommended to capture seismic actions in sites characterized by 2D-3D complex subsurface geometry and surface morphology (Pagliaroli et al., 2014; 2015). On the contrary, 1D effects (i.e. essentially the amplification of ground motion associated to soft horizontally layered sediments resting on bedrock) is usually addressed in the codes through standard elastic design spectra based on different soil categories, almost universally defined by the equivalent shear wave velocity in the upper 30 m ($V_{s,30}$). Amplification factors, defined for each soil category, are usually applied to the response spectrum defined at rock conditions (together with shape modifications) to consider 1D site effects. Moreover, nonlinear soil response is a key factor in controlling the amount of site amplification; for this reason, the amplification factors as well as the changes in spectral shape should be in principle related to the level of shaking. Recently, the increasing availability of numerical and instrumental data, allowed several studies aimed to suggest modifications in soil classification criteria (Pitilakis et al., 2013) and/or in amplification factors and response spectra adopted in the different codes (Pitilakis et al., 2013; Tropeano et al., 2018; Andreotti et al., 2013; Paolucci 2018).

In this paper the amplification factors specified by the Italian technical code NTC18 (Ministero delle Infrastrutture e dei Trasporti, 2018) are compared with empirical and analytical estimates of ground motion amplification. In particular, amplification factors for different soil conditions and intensity of input ground motion were computed by following two complementary approaches. A first set of "numerical" amplification factors was gathered from 1D numerical site response analyses carried out on virtual stratigraphic profiles in which lithology, shear

modulus and damping nonlinear curves, bedrock depth, shear wave velocity profiles, input motion were varied in prescribed ranges. A total number of 2760 of analyses were carried out with an equivalent linear approach; simulations associated to high shear strains were repeated with a true nonlinear code in order to overcome problems associated with the inaccuracy of numerical methods at high strains. A set of "empirical" amplification factors has been then derived by using almost 5600 selected recordings at about 100 downhole vertical arrays of the Kiban-Kyoshin Japanese network (Kik-net). The amplification factors were estimated by comparing ground motion recorded at soil surface and the corresponding motion at outcropping bedrock derived from recordings at depth in the array. The use of the Kik-net data was due to the lack of vertical array in the Italian network; here only a few recordings at pairs of nearby stations located at outcropping rock and soil conditions are available (Tropeano et al., 2018).

Nonlinear simplified relationship relating amplification factors to the level of shaking at rock were finally calibrated by using empirical and analytical estimates for different soil categories (B, C, D and E) as defined by NTC18 and compared with code relationships.

Even if restricted to NTC18 the approach followed can be regarded as general and the data here presented can be extended to the calibration of amplification factors having more general validity.

2 THE ITALIAN BUILDING CODE NTC18

This paper focuses on the Italian technical code NTC18 for which the spectrum at rock conditions (subsoil category A, Figure 1a) depends on 3 hazard parameters (a_g, F_0 and T_C^* in Figure 1b) defined over a grid of the Italian territory having a spatial resolution of about 5.5 km. Soil factors S_S and C_C, controlling amplitude and shape variations respectively (Figure 1b), are then introduced to define the standard response spectra for soil categories B-E (Figure 1) defined in terms of equivalent shear wave velocity $V_{S,eq}$:

$$V_{s,eq} = \frac{H}{\sum_{i=1}^{N} \frac{h_i}{V_{s,i}}} \tag{1}$$

being H the thickness of soil deposit, h_i and $V_{S,i}$ thickness and shear wave velocity of layer i, N the total number of soil layers. For H higher than 30 m, the equivalent velocity is computed by using H=30 in equation (1) thus obtaining the standard $V_{S,30}$.

For each soil category, soil factors are function of hazard parameters a_g, F_0 and T_C^* to consider soil nonlinearity (see inset in Figure 1b).

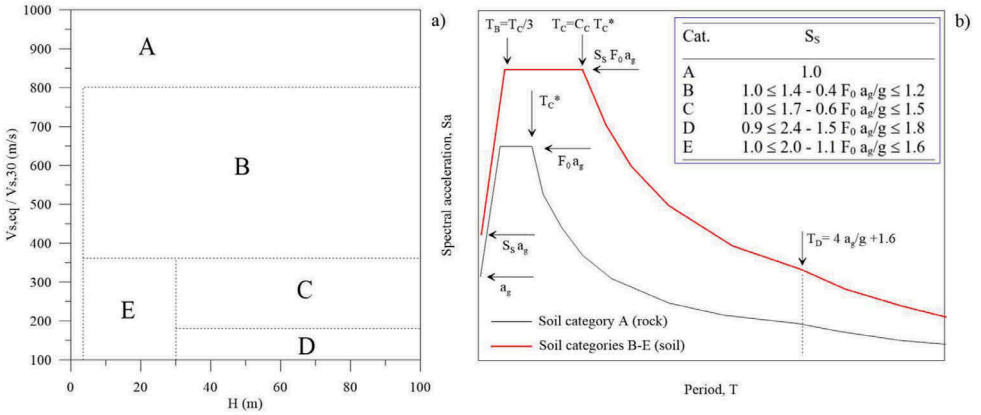

Figure 1. Soil categories (a) and meaning of hazard (a_g, F_0 and T_C^*) and soil (S_S and C_C) parameters (b) according to NTC18.

3 DATA AND METHODS

3.1 *Parametric site response analyses on virtual stratigraphic profiles*

The parametric 1D site response analyses were performed on a series of virtual deposits characterized by different lithologies (clay, sand, gravel) and wave velocity profiles representative of the B-C-D-E subsoil classes of the NTC18 (Figure 2). For classes C-D the thickness of soil deposit H was assumed equal to 40, 60 and 80 m while for B category also H = 20 m was explored; finally, for E category only H = 20 m was considered. For each subsoil class, except for D, different values of $V_{s,eq}$ or $V_{s,30}$ if H ≥30 m (e.g. 450 and 650 m/s for class B) were assumed in order to explore the variability associated with different V_S profiles. Regarding the nonlinear properties, for clay deposits (unit weight γ = 18 kN/m^3) the normalized shear modulus (G/G_0) and damping ratio (D) curves proposed by Vucetic and Dobry (1991) were considered, assuming plasticity index IP = 30. For the sands (γ=20 kN/m^3) and the gravels (γ=21 kN/m^3) the G/G_0 and D curves by Seed and Idriss (1970) and Rollins et al. (1998) were considered, respectively; moreover, for these soils, in order to take into account the increase in linearity and the reduction of dissipative properties with depth, the average curves of the proposed ranges were assumed in the first 30 m while for greater depth reference was made to the upper limit of the G/G_0 curve and to the lower one for the curve of D. For the seismic bedrock, γ=23 kN/m^3 and Vs = 800 m/s were assumed. Each virtual profile was then subjected to 60 pairs of natural accelerograms of increasing intensity recorded at outcropping of rock or very rigid soil. The accelerograms were divided into 6 classes, each consisting of 10 pairs, based on the maximum peak acceleration: 1-10 cm/s^2, 10-50 cm/s^2, 50-100 cm/s^2, 100-200 cm/s^2, 200-400 cm/s^2, > 400 cm/s^2. The accelerograms were extracted from the Italian ITACA database (http://itaca.mi.ingv.it/) and, for the higher energy classes, also from the international PEER database (https://ngawest2.berkeley edu/), assuming the following ranges for magnitude and distance: M=4.5-6.9, D=5-50 km. Overall 2760 parametric analyses were conducted with the equivalent linear mono-dimensional code STRATA (Kottke et al., 2013).

3.2 *Development of recordings database from Kik-net*

A total number of 93 stations of the KiK-net strong-motion network (http://www.kyoshin.bosai.go.jp/), each characterized by a vertical array comprising one surface and one in-hole seismometers, were analyzed. Based on subsoil conditions, each of them was assigned to one of the

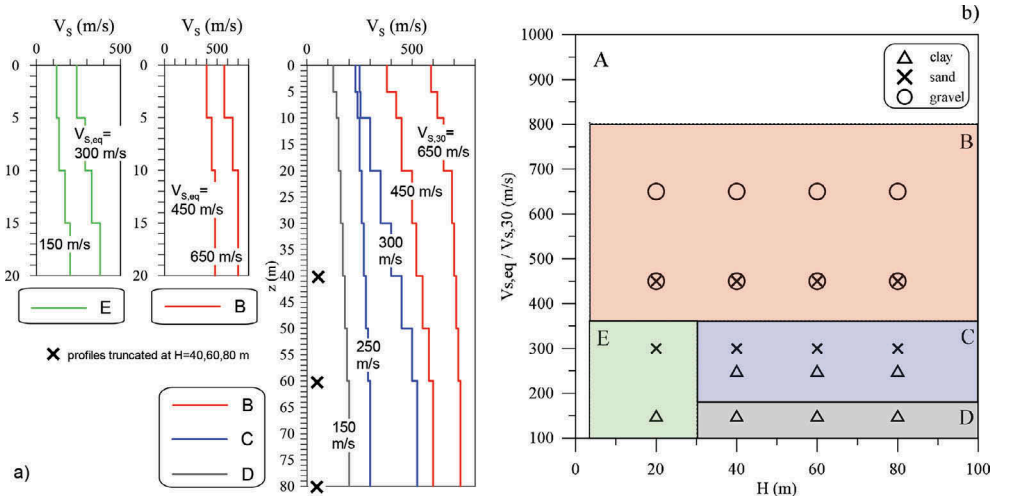

Figure 2. Range of shear wave profiles of virtual soil deposits considered for parametric analyses (a); NTC18 subsoil categories and corresponding classification of virtual deposits (b).

Table 1. Number of stations and accelerograms available for each NTC18 subsoil class extracted from KiK-net database for the present study (*pairs of simultaneous recordings at surface/deep sensors).

Soil category	recording stations	recordings*	maximum PGA_r
B	38	3458	0.71g
C	10	830	0.30g
D	2	140	0.10g
E	13	1158	0.31g
Total	**63**	**5586**	

classes of the NTC18. For each station, a database was compiled including: station name and code, $V_{S,30}$ (or $V_{S,eq}$), depth of the soil-bedrock interface z_{rock}, depth of the in-hole sensor z_s, shear wave velocity of the medium where the deep sensor is installed, summary description of the stratigraphy, V_S profile, available recordings. The number of recording stations and accelerograms available for each subsoil class are illustrated in Table 1. The 10 stations pertaining to subsoil class A are not included. Moreover, only the stations with Vs of the medium hosting the in-hole sensor higher than 750 m/s were considered, which led to not considering another 20 stations. The maximum Peak Ground Acceleration (PGA) at outcropping rock (PGA_r) computed as twice the PGA recorded at depth is also shown. Recordings having PGA_r lower than 0.01g and epicentral distances higher than 120 km were excluded. The table shows that not all subsoil classes are adequately represented: the subsoil class B has 38 stations with about 3500 recordings while class D has only 2 stations with a total of 140 registrations.

3.3 *Estimation of soil amplification factors*

The simplest way to estimate amplifications factor is to compare PGA at soil and rock sites. For the numerical analyses, S_S will therefore be computed as the ratio of PGA computed at soil surface and the corresponding parameter at outcropping bedrock. For empirical estimates, as said before, Kik-net recordings are available at surface and at depth within the bedrock. Considering that all the 93 stations were selected among those having in-hole sensor well below the rock-soil interface (i.e., $z_s > z_{rock} + 30m$) and assuming, as first approximation, that horizontal motion at depth is due to vertical incident shear waves, the PGA at outcropping bedrock was computed as double of the value recorded at depth. This assumption was verified with convolution analyses.

The amplification factors can be also evaluated considering the overall amplification of spectral amplitudes. In particular, a "global" amplification factor is calculated as ratio between the integral of 5% damped acceleration response spectrum, in the period range 0.05-2.5s, at soil (I_{soil}) and rock (I_{rock}) conditions. This ratio considers the amplification related to the increase of ordinates of soil spectra with respect to rock spectra, but also a contribution due to the change in shape. As is well known, average spectra for soils differ from those on rock because the high-amplitude spectral band becomes larger and shifted towards greater periods. The ratio I_{soil}/I_{rock} previously defined can be therefore represented as the product of the 'true' soil amplification coefficient S_S and a "shape ratio" SR reflecting only the difference between spectral shapes (Rey et al., 2002). In other words, $I_{soil}/I_{rock} = S_S * SR$ and the soil amplification factors can be therefore estimated as $I_{soil}/I_{rock} * (1/SR)$.

In general, the shape ratio SR can be estimated as following: the spectrum at soil conditions is first normalized by the corresponding PGA; then it is integrated over the period range 0.05-2.5s and divided by the same integral of normalized spectrum at rock site. Assuming the standard spectra defined in NTC18 for the subsoil categories (Figure 1b), the shape of soil spectrum is controlled by C_C parameter (Figure 1b) which in turn depend on hazard parameter T_C^* at rock conditions. As T_C^* slightly increases as a_g increases, it turns out that the shape ratio SR is not a constant but a function slightly decreasing as a_g increases; however, as first approximation, assuming an average T_C^*-a_g relationship calibrated on data referring to the whole national territory, a constant average value of SR can be computed for each soil category. These values

Table 2. Shape ratio SR computed for Eurocode 8 and NTC18 standard spectra and computed in the present study from numerical analyses (average SR from NTC are computed in the a_g=0.03-0.3g range).

Soil category	Eurocode 8		NTC18	Numerical (this study)
	type 1	type 2	(avg. 0.03-0.3g)	avg. ± σ
B	1.15	1.00	1.25	1.00 ± 0.12
C	1.27	0.99	1.34	1.22 ± 0.25
D	-	-	1.68	1.45 ± 0.47
E	-	-	1.49	1.07 ± 0.23

are reported in Table 2 together with the corresponding value derived from Eurocode type 1 (high seismicity) and type 2 (low-moderate seismicity) standard spectra and computed by Rey et al. (2002). SR from NTC18 are slightly higher than the Eurocode 8 ones meaning that in the Italian code the shifting in shape towards greater periods is more enhanced.

4 RESULTS AND DISCUSSION

4.1 *Numerical amplification factors*

The results of the parametric analyses are shown in Figure 3 in terms of variation of the stratigraphic amplification coefficient Ss with the input PGA_r (at outcropping bedrock, a_g in NTC18) for each of the 4 subsoil classes (B-E). As expected, for all the categories a general reduction of Ss is observed as the intensity of the input motion increases due to the nonlinear soil behavior.

The dataset of amplification factors was processed to obtain a simple relationship between S_S and PGA_r. For each subsoil class a simple exponential law $S_S = a\, e^{b*PGAr}$ was first used; moreover, a piecewise constant-power relationship (Tropeano et al., 2018) was employed:

$$S_S = m \quad \text{for } PGA_r \leq x_i \quad \text{and} \quad S_S = \frac{a(PGA_r - x_0)^b}{PGA_r} \quad \text{for } PGA_r > x_i$$

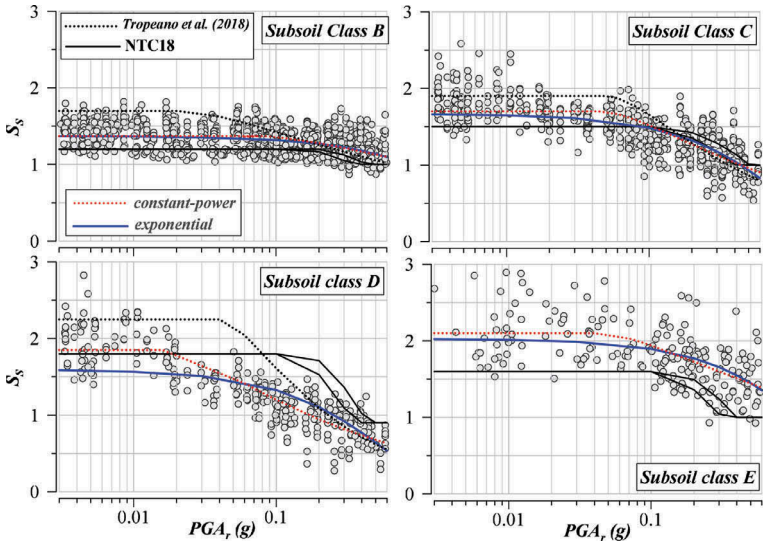

Figure 3. Numerical stratigraphic amplification factors in terms of PGA for subsoil categories B-E and comparison with NTC18 provisions and literature data.

Table 3. Coefficients of the relationships expressing the nonlinear behavior of amplification factors S_S.

Soil category	Exponential		Constant-power piecewise					
		R^2	m	a	b	x_0	x_i	R^2
B	$S_S=1.37\ e^{-0.37\ PGAr}$	0.25	1.37	1.026	0.828	0.013	0.075	0.21
C	$S_S=1.67\ e^{-1.165\ PGAr}$	0.62	1.70	0.773	0.660	0.015	0.044	0.60
D	$S_S=1.60\ e^{-1.825\ PGAr}$	0.62	1.85	0.526	0.625	0.006	0.016	0.77
E	$S_S=2.03\ e^{-0.673\ PGAr}$	0.35	2.10	1.256	0.780	0.009	0.040	0.38

The best-fit parameters for both relationships are reported in Table 3 with the corresponding coefficient of determination R^2 while the curves are reported in Figure 3 together with: i) NTC18 provisions (computed from the expressions of S_S in Figure 1b for two F_0 limit values 2.3 and 2.9) and ii) relationships found by Tropeano et al. (2018) on the basis of parametric 1D analyses similar to those presented in this paper, as well as on empirical and semi-empirical estimates based on the processing of recordings of seismic events in well-characterized recording stations of the Italian seismic network. The use of the constant-power relationship allows to slightly improve the fitting of numerical data for subsoil classes D and E (see R^2 in Table 3); however, the simple exponential law is generally satisfactory for practical purposes.

Comparing the numerical S_S-PGA_r relationships with the NTC provisions, a substantial agreement for the subsoil classes B and C is observed, even if for low levels of input intensity, the S_S of NTC systematically underestimate the amplifications obtained numerically. The NTC upper limits (1.2 and 1.5 for the categories B and C, respectively) would therefore appear slightly non-conservative: the numerical analyses suggest values of about 1.4 and 1.7 at low PGA (Figure 3 and Table 3). In contrast, for subsoil classes D and E there is a noticeable discrepancy between NTC provisions and the results of parametric numerical analyses. For class D the analyses provide values of Ss well below those by NTC throughout the range of input PGA. As far as class E is concerned, the numerical Ss, despite the high dispersion of the points, appear quite higher than those provided by NTC. Since the class D deposit is the softest one, it is possible that this discrepancy between numerical and NTC amplification factors is in some way due to the lack of reliability of the equivalent linear method at high shear strains (Kaklamanos et al., 2013). True nonlinear analyses were then performed with Deepsoil (Hashash et al., 2017) on D profiles, for 200-400 cm/s^2 and > 400 cm/s^2 input classes; no significant differences in terms of Ss were observed with respect to the equivalent linear approach.

The comparison between the results of the present study and that of literature shows finally a good agreement for PGA input> 0.1-0.2g, while below this range the Ss estimated by Tropeano et al. (2018) are significantly higher. This overestimation is partly because the literature study includes empirical and semi-empirical estimates, particularly abundant for PGA <0.1g, which generally provide higher amplifications than numerical studies on ideal profiles.

The amplification factors considering the overall amplification of spectral amplitudes in the 0.05-2.5 s period range are reported in Figure 4 in terms of average trends expressed via the best fit exponential law. The "global" amplification factor I_{soil}/I_{rock}, considering both the increase of ordinates of soil spectra and the change in shape, as expected, is placed above the normative values except for subsoil class D where numerical and code values are almost comparable. Assuming the NTC18 standard spectra and the corresponding average SR reported in Table 2, the "spectral" S_S were computed as I_{soil}/I_{rock} * (1/SR).

These amplification factors are significantly lower than both NTC provisions and S_S calculated in terms of PGA, in the whole input range and for all subsoil classes. This underestimation can be attributed to an overestimation of SR by the NTC spectra as confirmed by the comparison between average SR from standard NTC spectra and the SR values calculated on the normalized spectra obtained from numerical analyses (Table 2) which are in turn more in line with the shape factors suggested by the Eurocode8. The numerical analyses therefore show that the NTC seems to predict an excessive enlargement of the spectra towards the high periods for all the subsoil classes due to an overestimation of the SR factors and therefore of the C_C parameters. A similar consideration has recently been presented by other authors (e.g., Aimar et al., 2018).

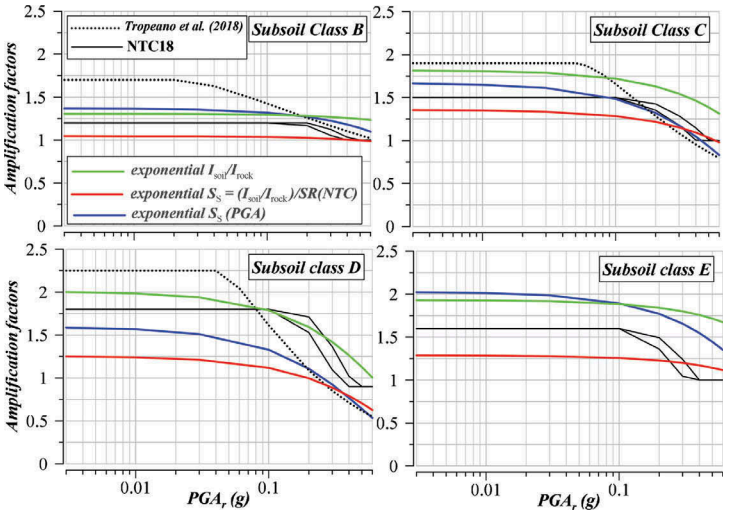

Figure 4. Estimation of amplification factors from spectrum intensities for subsoil categories B-E and comparison with NTC18 provisions and literature data.

4.2 *Empirical amplification factors*

The variation of empirical stratigraphic amplification coefficient S_S in terms of PGA with the input PGA_r is shown in Figure 5. As for numerical factors, the dataset of values was processed using both exponential and piecewise constant-power fitting relationships. Here reference is made only to constant-power functions which allow a better agreement with data. Moreover, the NTC18 provisions as well as numerical S_S trend found in this study (constant-power fitting) and numerical-empirical functions provided by Tropeano et al. (2018) are reported for comparison.

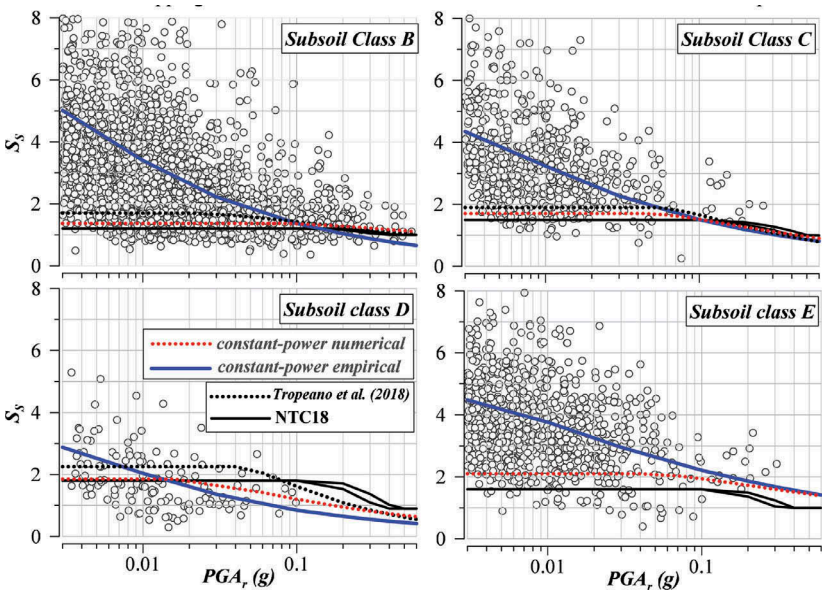

Figure 5. Estimation of empirical stratigraphic amplification factors in terms of PGA from KiK-net recordings for subsoil categories B-E and comparison with numerical estimates, NTC18 and literature data.

The empirical values generally show high dispersion, especially at low PGA_r values where the amplification factors are sensitively higher than those numerically predicted. At higher PGA_r empirical data meet numerical ones except for soft soil class D where they show a higher degree of nonlinearity. The reason for these differences is most probably due to the high Vs of the material in which the deep sensor is located, generally far greater than the 800 m/s used as a reference for the definition of the stratigraphic amplification in the NTC code and in the numerical schemes: half of the sensors (51%) are installed in rock having $V_S > 2000$ m/s, about 30% of sensors has $V_S = 1200$-2000 m/s. At low PGA_r (i.e., in the linear range) the higher impedance contrast associated to empirical estimates lead to higher amplification factors; at the same time, at high PGA_r this implies a more pronounced nonlinearity in the softest deposit (i.e., class D).

Numerical and empirical S_S estimates are therefore not directly comparable. In order to overcome these difficulties, 1D analyses are currently in progress on all the considered KiK-net stations. The idea is to extrapolate the ground motion in correspondence of a "virtual" sensor located at the outcropping of a formation with V_S ~800 m/s to be used as reference to compute S_S

5 CONCLUSIONS

Nonlinear stratigraphic amplification factors S_S were derived from a large set of numerical 1D site response analyses carried out on virtual soil profiles as well as from the processing of more than 5500 recordings from Japanese KiK-net stations. The aim was to assess the performance of S_S as specified by the Italian code NTC18. The stratigraphic factors were computed in terms of PGA as well as ratio of integral spectral amplitude in the range of period 0.05-2.5s.

The results of parametric numerical analyses indicate that for subsoil classes B and C the amplification factors prescribed by NTC18 perform satisfactorily, even if they appear slightly non-conservative at low input PGA. On the contrary, for the softer class D and class E, the amplification factors provided by NTC18 severely overestimate and underestimate the response, respectively. Moreover, the results show that NTC foresees an excessive enlargement of the spectra towards high periods for all the classes due to an overestimation of the shape C_C parameter.

The empirical values, derived from KiK-net data in terms of PGA, generally show high dispersion, especially at low input values where the amplification factors are quite higher than numerical ones. At higher PGA_r empirical data meet numerical ones except for soft class D showing a higher degree of nonlinearity. The high Vs of bedrock in the KiK-net stations, well above the 800 m/s assumed for numerical schemes and in the NTC18, has been invoked to explain these discrepancies. Numerical convolution 1D analyses are currently in progress on KiK-net profiles to refer the amplification factors to a Vs=800 m/s making homogeneous empirical and numerical estimates. Merging these data will allow to calibrate S_S nonlinear relationships.

REFERENCES

Aimar M., Ciancimino A., Foti S. 2018. Valutazione dei metodi semplificati proposti nelle NTC18 per la stima degli effetti di sito: un approccio stocastico. *Proc. IARG 2018* (in italian)

Andreotti G., Famà A., Lai C.G. (2018). Hazard-dependent soil factors for site-specific elastic acceleration response spectra of Italian and European seismic building code. *Bull. Earth. Eng*. 16, 5769–5800.

CEN (European Committee for Standardization) 2004. Eurocode 8: Design of structures for earthquake resistance, Part 1: general rules, seismic actions and rules for buildings. EN1998–1:2004. Brussels.

Hashash, Y.M.A., Musgrove, M.I., Harmon, J.A., et al. 2017. DEEPSOIL 7.0, User Manual.

Kaklamanos J., Bradley B.A., Thompson E.M., Baise L.G. 2013. Critical Parameters Affecting Bias and Variability in Site-Response Analyses Using KiK-net Downhole Array Data. *Bull. Seism. Soc. Am*. 103(3):1733–1749.

Kottke A. R., Wang X., Rathje E. M. 2013. Technical Manual for Strata. *Geotechnical Engineering Center, Dep. of Civil, Architectural, and Environmental Engineering, University of Texas*, 89 pp.

Ministero delle Infrastrutture e dei Trasporti (2018). D.M. 17/ 01/2018.Aggiornamento delle «Norme Tecniche per le Costruzioni».

NEHRP, 1991. Recommended Provisions for the Development of Seismic Regulations for New Buildings, *Buildings Seismic Safety Council for Federal Emergency Management Agency*, Washington DC.
Paolucci R. 2018. Site classification and site effects in the seismic norms: work in progress for the revision of Eurocode8. *Proc. XXV ciclo Conferenze Geotecniche di Torino (CGT)*, Politecnico di Torino.
Pagliaroli A., Quadrio B., Lanzo G., Sanò T. 2014. Numerical modelling of site effects in the Palatine hill, Roman Forum and Coliseum archaeological area. *Bull. Earth. Eng*. 12, 1383–1403.
Pagliaroli A., Avalle A., Falcucci E., Gori S., Galadini F. 2015. Numerical and experimental evaluation of site effects at ridges characterized by complex geological setting. *Bull. Earth. Eng*., 13:2841–2865.
Pitilakis K, Riga E, Anastasiadis A. 2013. New code site classification, amplification factors and normalized response spectra based on a worldwide ground-motion database. *Bull Earthq Eng*. 11, 925–966.
Rey, J., Faccioli, E., & Bommer, J. J. 2002. Derivation of design soil coefficients (S) and response spectral shapes for Eurocode 8 using the European Strong-Motion Database. *J. Seismology* 6: 547–555.
Rollins, K. M., Evans, M. D., Diehl, N. B., Daily III, W. D. 1998. Shear modulus and damping relationships for gravels. *Journal of Geotechnical and Geoenvironmental Engineering*, 124(5): 396–405.
Seed H.B., Idriss I.M. 1970. Soil moduli and damping factors for dynamic response analyses. *Technical Report EERRC-70-10*, *University of California*, *Berkeley*.
Tropeano G., Soccodato F.M., Silvestri F. (2018). Re-evaluation of code-specified stratigraphic amplification factors based on Italian experimental records and numerical seismic response analyses. *Soil Dyn. Earth. Eng*., 110, 262–275.
Vucetic, M., Dobry, R. 1991. Effects of the soil plasticity on cyclic response. *J. Geot. Eng. Div*. 117,89–107.